Dynamics of the UvrABC Nucleotide Excision Repair Proteins Analyzed by Fluorescence Resonance Energy Transfer

Erik Malta, Geri F. Moolenaar, and Nora Goosen*

Laboratory of Molecular Genetics, Leiden Institute of Chemistry, Gorlaeus Laboratories, Leiden University, Einsteinweg 55, 2333 CC Leiden, The Netherlands

Received February 2, 2007; Revised Manuscript Received May 15, 2007

ABSTRACT: UvrB plays a key role in bacterial nucleotide excision repair. It is the ultimate damage-binding protein that interacts with both UvrA and UvrC. The oligomeric state of UvrB and the UvrAB complex have been subject of debate for a long time. Using fluorescence resonance energy transfer (FRET) between GFP and YFP fused to the C-terminal end of *Escherichia coli* UvrB, we unambiguously show that in solution two UvrB subunits bind to UvrA, most likely as part of a $UvrA_2B_2$ complex. This complex is most stable when both UvrA and UvrB are in the ATP-bound form. Analysis of a truncated form of UvrB shows that binding to UvrA promotes dimerization of the two C-terminal domain 4 regions of UvrB. The presence of undamaged DNA leads to dissociation of the $UvrA_2B_2$ complex, but when the ATPase site of UvrB is inactivated, the complex is trapped on the DNA. When the complex is bound to a damaged site, FRET between the two UvrB subunits could still be detected, but only as long as UvrA remains associated. Dissociation of UvrA from the damage-bound UvrB dimer leads to the reduction of the magnitude of the FRET signal, indicating that the domain 4 regions no longer interact. We propose that the UvrA-induced dimerization of the domain 4 regions serves to shield these domains from premature UvrC binding. Only after specific binding of the UvrB dimer to a damaged site and subsequent release of UvrA is the contact between the domain 4 regions broken, allowing recruitment of UvrC and subsequent incisions.

Nucleotide excision repair (NER)[1] in prokaryotes involves the NER-specific proteins UvrA, UvrB, and UvrC (*1*−*3*). Damage-specific DNA binding is achieved by a complex of UvrA and UvrB. Initially, distortions in the DNA helix are detected by UvrA, after which the presence of a lesion is verified by UvrB. This finally leads to stable binding of UvrB to the damaged site and release of UvrA. The UvrB−DNA preincision complex is subsequently bound by UvrC, resulting in two incisions, one on either side of the lesion. The UvrA and UvrB proteins contain two ATP binding sites and one ATP binding site, respectively, and the binding and hydrolysis of ATP play important roles during the different steps of the repair reaction (*1*). Crystal structures of UvrB from different organisms (*4*−*6*) revealed that UvrB consists of five domains, namely, 1a, 1b, 2, 3, and 4 (Figure 1A,B). The C-terminal domain (domain 4), which is connected to the remainder of the protein via a flexible linker, is not visible in the crystal structure of the full-length protein, but its structure has been determined separately (*7*, *8*). The ATP cofactor is sandwiched between domains 1a and 3. Domain 2 was shown to be essential for interaction with UvrA (*9*), and a second UvrA binding site was identified in a maltose binding protein fusion containing domain 4 and part of domain 3 (*10*).

The oligomeric states of the UvrA and UvrB proteins from *Escherichia coli* have been determined with different techniques. Gel filtration (*11*) and sedimentation experiments (*12*) indicated that UvrA forms a dimer in solution and that this dimer is stabilized by the binding of ATP. Similar experiments with UvrB initially showed this protein to be a monomer in solution (*11*), but at relatively high protein concentrations (micromolar range), UvrB dimers could be detected (*13*). The stoichiometry of UvrAB complexes in solution has been the subject of debate for a long time. From isolation of UvrAB complexes and subsequent analysis of their protein content on a denaturing protein gel, a UvrA/UvrB ratio of 1.8 was calculated, from which it was suggested that the complexes consist of two UvrA molecules and one UvrB molecule (*11*). Determining the size of UvrAB complexes bound to undamaged DNA by atomic force microscopy (AFM), however, showed that the UvrAB complex in search of damage contains two UvrA and two UvrB subunits (*14*), suggesting that also in solution a $UvrA_2B_2$ complex is formed. Finally, AFM (*14*) and gel retardation analysis (*15*) have shown that the UvrB preincision complex formed upon damage recognition consists of two UvrB subunits, with one subunit stably associated with the damaged site and the other more loosely bound. This again is a strong indication that the active UvrAB complex that initially binds the damage contains two UvrB subunits.

The C-terminal domain (domain 4) of UvrB stabilizes the UvrB dimer, both in solution (*13*) and on the DNA (*14*, *15*). The separately isolated domain 4 was shown to dimerize both

* To whom correspondence should be addressed. Phone: 31-715274773. E-mail: N.Goosen@chem.leidenuniv.nl.

[1] Abbreviations: NER, nucleotide excision repair; FRET, fluorescence resonance energy transfer; GFP, green fluorescent protein; YFP, yellow fluorescent protein; CK, creatine kinase; CP, creatine phosphate; PDB, Protein Data Bank.

10.1021/bi7002235 CCC: $37.00
Published on Web 07/14/2007

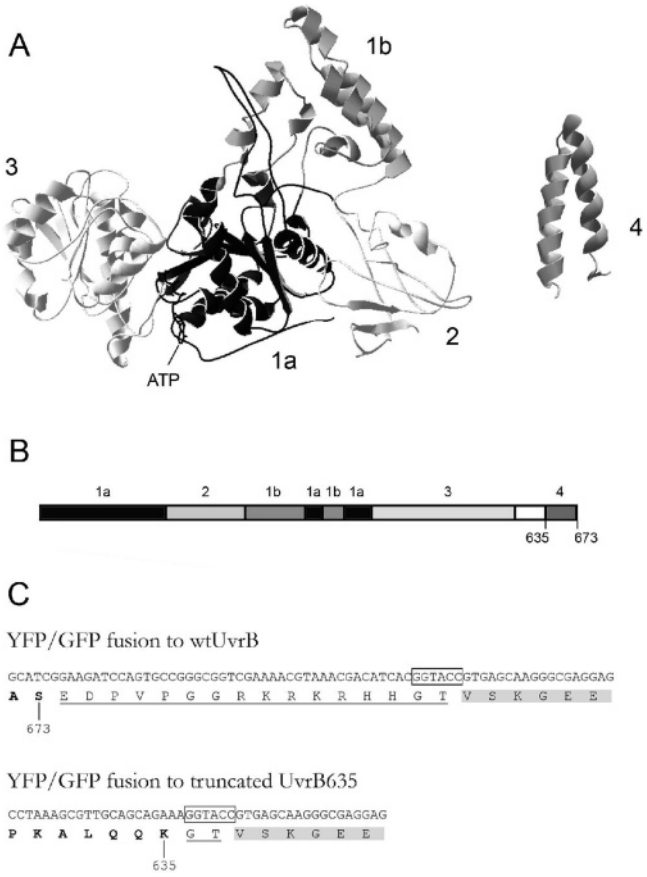

FIGURE 1: (A) Crystal structure of the UvrB protein (PDB entry 1D9Z) and the separate C-terminal domain 4 (PDB entry 1Q0J). The different domains of the protein (1a, 1b, 2, 3, and 4) are indicated. The ATP molecule that is sandwiched between domains 1a and 3 is shown. (B) Linear representation of the UvrB protein. The domains are colored black (1a) and different shades of gray (2, 3, and 4). The flexible linker that separates domain 4 from domain 3 is colored white. The positions of the GFP and YFP fusion points (635 and 673) are indicated. (C) Amino acid sequence of the UvrB−YFP and −GFP joints of the fusion proteins. The YFP and GFP parts are highlighted in gray. The linker sequences are underlined, and the UvrB sequences are shown in bold.

in crystals (*7*) and in solution (*8*). In the absence of domain 4, however, dimers of UvrB in solution or on the DNA can still be found, albeit with reduced frequency, indicating that there are additional contacts in the UvrB dimer besides those in domain 4 (*13*, *14*).

The UvrC protein consists of two functional halves, with the catalytic site for 3′ incision located in the N-terminal part and the catalytic site for 5′ incision in the C-terminal part (*16*, *17*). The N-terminal half also contains a domain that is homologous to domain 4 of UvrB. Mutational analysis revealed that interaction of the homologous domains of UvrB and UvrC is required for 3′ incision (*18*, *19*). Addition of UvrC to UvrB dimers bound to a lesion was shown to lead to dissociation of one of the UvrB subunits from the DNA (*15*).

In this paper, we have monitored the *E. coli* UvrB dimerization by fluorescence resonance energy transfer (FRET) between GFP and YFP fused to the C-terminal end of UvrB. We find that in the absence of UvrA no detectable FRET signal is obtained. Upon addition of UvrA, however, a strong FRET signal is observed, showing for the first time that the UvrAB complex in solution contains two UvrB proteins in spatial proximity, most likely as part of a $UvrA_2B_2$ complex. The dynamics of this complex was further analyzed by assessing FRET in the presence of different cofactors and/or undamaged and damaged DNA.

EXPERIMENTAL PROCEDURES

Cloning, Expression, and Purification of the GFP−YFP Fusion Proteins. GFP2 is a GFP variant with excitation (396 nm) and emission (509 nm) comparable to those of wild-type GFP but with a F64L substitution that increases the brightness significantly (Perkin-Elmer, Inc., Dreieich, Germany). It has been shown to form a good FRET pair with eYFP (GFP with S65G, V68L, S72A, and T203Y substitutions) which has an excitation optimum at 513 nm and emission at 527 nm (*20*). To avoid sterical hindrance of the GFP−YFP fusion on the function of domain 4, we chose to fuse the fluorescent proteins to the C-terminus of UvrB via a 16-amino acid linker (Figure 1C). The sequence of this linker was derived from a naturally occurring C-terminal extension of the *Thermus aquaticus* UvrB. First, a DNA fragment encoding this linker and containing a KpnI site was fused to the UvrB coding region of pNP83 via PCR. Next the GFP2 and eYFP coding regions were amplified via PCR via introduction of a KpnI site at the N-terminus (adding another glycine and threonine residue to the linker) and a HindIII site after the stop codon. Finally, the KpnI−HindIII PCR fragment was inserted into the pNP83 derivative mentioned above. For isolation of the GFP−YFP fusions lacking domain 4, a KpnI site was introduced after the codon encoding L635 in pNP83. Next, the same PCR fragments with the GFP2 and eYFP coding regions were ligated in this pNP83 derivative. Since residues 600−635 already form a flexible linker region (which normally separates domain 4 from the "body" of the UvrB protein), no additional linker fragment was added to this construct. All constructs were verified for the absence of PCR-induced mutations by DNA sequencing. The sequences of the different fusion constructs are shown in Figure 1C. For production of the fusion proteins with an inactive ATPase site (K45A), the corresponding mutation (described in ref *21*) was inserted into the fusion plasmids via restriction fragment exchange. The fusion proteins were expressed in CS5017 (GM1, Δ*uvrB*) which has been described (*22*). For purification of the mutant proteins, the same procedure that was used for wtUvrB (*23*) was employed.

Proteins, Chemicals, and DNA Substrates. Creatine kinase (CK), creatine phosphate (CP), ADP (containing <1% ATP), ATP (containing <0.5% ADP), and ATPγS (containing <10% ADP) were obtained from Roche. The *E. coli* proteins UvrA (*24*), UvrB (*23*), and UvrC (*24*) were purified as described previously. A DNA construct expressing UvrC-(E81A) was constructed by site-directed mutagenesis, and the mutant protein was purified according to the same protocol as wtUvrC. The 50 bp DNA fragment containing a N3-menthol lesion at position 27 (*25*) was labeled at the 5′ side of the top strand using polynucleotide kinase as described previously (*24*). To study the effect of DNA on the FRET measurements, we used 1 μg of the Generuler DNA ladder mix (Fermentas) which is a mixture of linear DNA fragments ranging in size from 100 to 10 000 bp. To obtain DNA with UV lesions, the same mixture of DNA fragments was irradiated with 1000 J/m^2, which yields ~1

pmol of UV lesions for 1 μg of DNA (*26*). For filter binding assays, the same DNA ladder mix was first treated with alkaline phosphatase and next ^{32}P-labeled with T4 polynucleotide kinase as described previously (*27*).

UvrABC Incision Assay. The labeled 50 bp DNA substrate (2 fmol) containing a N3-menthol lesion (*28*) was incubated with 2.5 nM UvrA, 100 nM UvrB (or fusion protein), and 25 nM UvrC in 20 μL of Uvr-endo buffer [50 mM Tris-HCl (pH 7.5), 100 mM KCl, 10 mM $MgCl_2$, 0.1 μg/μL BSA, and 1 mM ATP]. After 30 min, the reaction was stopped by adding 2 μL of 2 μg/mL glycogen followed by ethanol precipitation. The incision products were visualized on a 15% denaturing acrylamide gel.

FRET Measurements. For FRET measurements of proteins in solution, 60 μL samples containing 25 pmol of UvrB (UvrB−GFP2 and UvrB−eYFP in a ratio of 1:9) and 25 pmol of UvrA were incubated in Uvr-endo buffer with or without the indicated cofactor at 1 mM for 10 min at 37 °C. After incubation, the sample was transferred to a 3 mm × 3 mm quartz cuvette and the cuvette placed in the cuvette holder of the fluorimeter. Fluorescence emission spectra were obtained using a Perkin-Elmer LS 50B fluorimeter, which was connected to a temperature-variable water bath to maintain a temperature inside the cuvette of 37 °C. The excitation wavelength was set at 396 nm (excitation of GFP2) with the excitation slit width at 5 nm. The scan range was from 450 to 550 nm at a scan speed of 400 nm/min with an emission slit width of 5 nm. For each incubation, five accumulative scans were performed. For FRET measurements in the presence of DNA 0.17 μg/μL CK and 20 mM CP together with 1 μg of DNA were added to the incubation described above. For FRET measurements in the presence of UvrC, the UvrA and UvrB proteins were first incubated with DNA and the ATP-regenerating system for 10 min at 37 °C. Next, 25 pmol of (mutant) UvrC was added, and the mixture was incubated for an additional 15 min to allow incision. To correct for eYFP emission due to direct excitation at 396 nm for each incubation, a control acceptor spectrum in a case where the GFP2 fusion was replaced by the wtUvrB protein was recorded. The resulting emission spectrum was subtracted from the emission spectrum of the donor/acceptor pair. To determine the relative amount of FRET, the *E*(527)/*E*(509) ratio of each donor/acceptor sample was divided by the ratio of the same incubation with the donor alone (i.e., where the eYFP fusion was replaced with wtUvrB). The values presented in this paper are the average of at least three independent spectra from which the direct eYFP emission spectrum was subtracted.

Filter Binding Assay. The filter binding assays were conducted using exactly the same conditions that were used for the FRET assays. Samples (60 μL) containing 25 pmol of UvrB (UvrB−GFP2 and UvrB−eYFP in a ratio of 1:9) and 25 pmol of UvrA were incubated with 1 μg of (irradiated) ^{32}P-labeled DNA in Uvr-endo buffer containing 1 mM ATP, 0.17 μg/μL CK, and 20 mM CP for 10 min at 37 °C. Next, when indicated, 25 pmol of UvrC was added and the incubation continued for an additional 15 min, after which 1.5 mL of ice-cold 2×SSC (0.3 M NaCl and 0.03 M trisodium citrate) was added. The mixture was poured over a nitrocellulose filter; the incubation vial was rinsed with 1 mL of 2×SSC, and finally, the filters were washed with 1.5 mL of 2×SSC. Each sample was corrected for the amount of DNA retained on a filter in the absence of protein. Binding is expressed as the percentage of the input DNA retained on the filter.

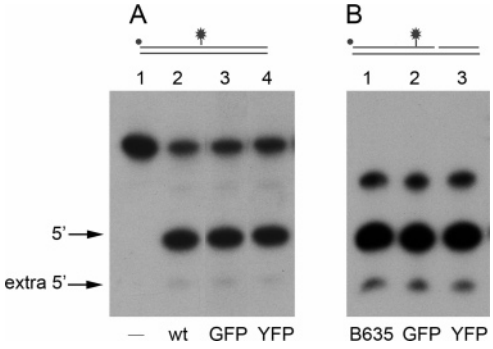

FIGURE 2: UvrABC incision on a 5′ terminally labeled 50 bp substrate with an N3-menthol lesion. (A) The 50 bp substrate was incubated with UvrA, UvrC, and no UvrB (lane 1), wtUvrB (lane 2), UvrB−GFP (lane 3), or UvrB−YFP (lane 4). (B) The same substrate which is now prenicked at the 3′ incision site was incubated with UvrA, UvrC, and UvrB635 (lane 1), UvrB635−GFP (lane 2), or UvrB635−YFP (lane 3). The 5′ incision products are denoted with arrows.

RESULTS

Isolation of UvrB−GFP2 and UvrB−eYFP Fusion Proteins. Fluorescent resonance energy transfer (FRET) between an excited donor molecule and an acceptor molecule depends inversely on the sixth power of the distance between the two fluorophores and can therefore be used to test whether two molecules are in spatial proximity. We have used the FRET pair GFP2 and eYFP to analyze the monomer−dimer state of the UvrB protein during the different steps of the repair reaction. The two GFP derivatives were fused to the C-terminal part of the UvrB protein via a linker as described in Experimental Procedures (Figure 1C). Both fusions fully complemented a Δ*uvrB* strain for UV resistance (not shown), indicating that the GFP−YFP moieties do not interfere with UvrB activity during repair. This was confirmed in vitro with the purified proteins. The UvrABC-mediated incision of a 50 bp DNA fragment containing a N3-menthol lesion is comparable in the presence or absence of the GFP−YFP fusions (Figure 2).

FRET Measurements of UvrB and UvrAB Complexes. To monitor the dimerization of UvrB in solution, the GFP2 and eYFP fusions were mixed and fluorescence emission spectra were recorded. A FRET signal can only be observed when the majority of the donor UvrB−GFP2 molecules are bound to the UvrB−eYFP acceptor. To achieve this, the acceptor (eYFP) was added in excess to the donor (GFP2). The ratio of GFP2 to eYFP was varied from 1:5 to 1:30. An example of such a spectrum is shown in Figure 3A. None of the conditions that were used gave rise to a significant FRET signal. Neither the addition of ATP, ADP, or ATPγS (Table 1) nor lowering the temperature to 4 °C (not shown) resulted in a significant difference in the emission spectrum. Apparently, the amount of UvrB dimers in solution is too low to be detected by this technique, or the GFP and YFP proteins are too far separated in the UvrB dimer to allow FRET.

When UvrA and ATP were added to our UvrB mixture, a FRET signal was obtained which can be seen from the decrease in the magnitude of the donor signal (509 nm) and

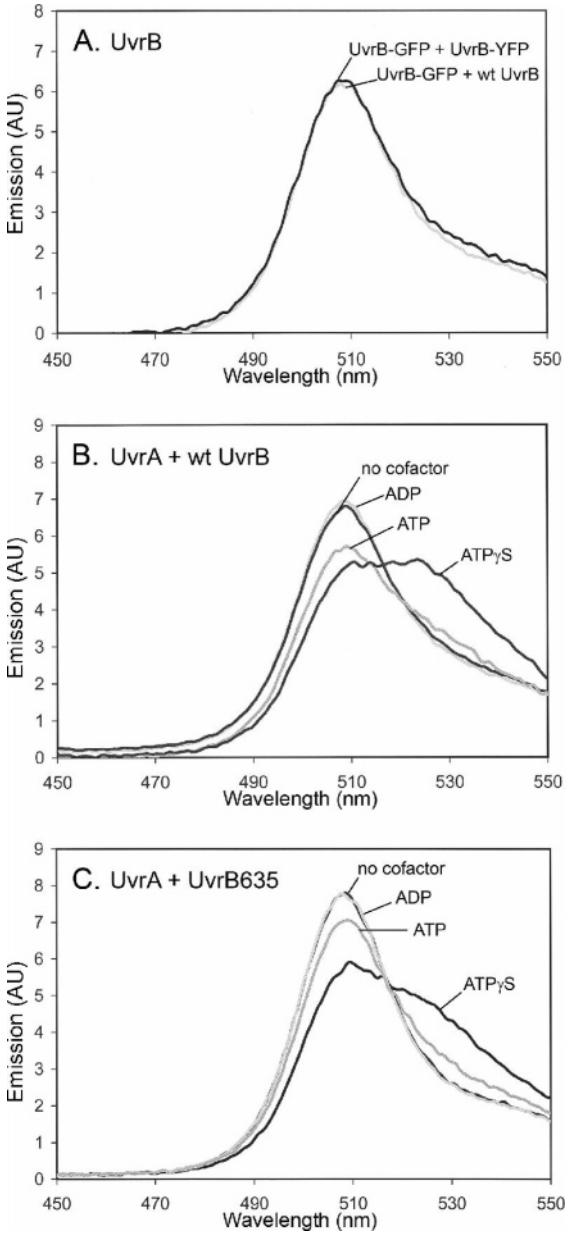

FIGURE 3: Emission spectra of the UvrB−GFP/UvrB−YFP pair. (A) UvrB−GFP (2.5 pmol) was mixed with 22.5 pmol of UvrB−YFP in UV-endo buffer with 1 mM ATP. (B) UvrB−GFP (2.5 pmol) was mixed with 22.5 pmol of UvrB−YFP and 25 pmol of UvrA without cofactor (black) or with 1 mM ADP (light gray), 1 mM ATP (dark gray), or 1 mM ATPγS (black). (C) UvrB635−GFP (2.5 pmol) was mixed with 22.5 pmol of UvrB635−YFP and 25 pmol of UvrA without cofactor (black) or with 1 mM ADP (light gray), 1 mM ATP (dark gray), or 1 mM ATPγS (black). Spectra were recorded (in arbitrary units) at 37 °C with excitation at 396 nm (excitation of GFP2). The spectra have been corrected for the direct emission of YFP at 396 nm by subtracting the spectra of protein mixtures containing 2.5 pmol of wtUvrB mixed with 22.5 pmol of UvrB−YFP (with or without UvrA and indicated cofactors).

the increase in the magnitude of the acceptor signal (527 nm) (Figure 3B). Apparently, UvrA can bring two UvrB molecules into spatial proximity, showing that in solution two UvrB molecules can bind to UvrA. Since UvrA has been shown to form a dimer in solution, it is most likely that the FRET-positive complex is a $UvrA_2B_2$ complex. The FRET signal was optimal when a GFP2:eYFP ratio of 1:9 was used. This ratio was used in all further experiments. When UvrA and UvrB were incubated without cofactor or with ADP, the 527 nm:509 nm emission ratio was not significantly different from the emission ratio of the GFP donor alone (Figure 3B and Table 1), showing that under these conditions there is no detectable FRET. When ATP together with the ATP-regenerating system (CP/CK) was added to the proteins, the level of FRET is higher compared to that with ATP alone (Table 1). In the presence of the nonhydrolyzable cofactor ATPγS, the FRET signal is even further increased (Figure 3B and Table 1). Apparently, FRET is optimal when the $UvrA_2B_2$ complex is in the ATP-bound form.

Table 1: Relative FRET Values of Proteins in Solution

	UvrB	UvrAB	UvrAB(K45A)	UvrAB635
no cofactor	1.07 ± 0.03	1.05 ± 0.03	nd	0.92 ± 0.04
ADP	1.08 ± 0.02	1.05 ± 0.02	0.92 ± 0.05	0.92 ± 0.05
ATP	1.05 ± 0.03	1.44 ± 0.06	1.62 ± 0.08	1.22 ± 0.02
ATP and CP/CK	nd	1.95 ± 0.06	1.73 ± 0.04	1.52 ± 0.09
ATPγS	1.06 ± 0.03	2.29 ± 0.06	1.95 ± 0.07	1.98 ± 0.09

ATP Hydrolysis by UvrA and UvrB Reduces the Magnitude of the FRET Signal. To test whether it is the ATPase activity of UvrA or that of UvrB that is responsible for reducing the magnitude of the FRET signal, we next introduced the K45A mutation into the UvrB−GFP2 and UvrB−eYFP fusion proteins. This mutation in the Walker A motif of the ATP binding site blocks ATP hydrolysis by UvrB and prevents formation of the preincision complex (ref *29* and our results not shown). The magnitude of the FRET signal of the UvrAB complex with the K45A mutation in the presence of ATP is higher (1.62) compared to that of the wild-type complex (1.44) (Table 1), indicating that the ATPase activity of UvrB results in a lower level of FRET. In the presence of ATPγS, however, the magnitude of the signal is further increased [1.95 (Table 1)]. Since UvrB-(K45A) cannot hydrolyze ATP, this difference between ATP and ATPγS must reflect the ATPase activity of UvrA. Taken together, these results indicate that in solution both UvrA and UvrB hydrolyze ATP and that this ATP hydrolysis by both proteins leads to a reduction of the magnitude of the FRET signal, most likely as a consequence of partial or complete dissociation of the $UvrA_2B_2$ complex.

When the ATP-regenerating system (CP/CK) is added to the UvrAB(K45A) complex again, the level of FRET is higher compared to that with ATP alone, and with ATPγS, it is further increased which was seen for the wild-type complex (Table 1). The FRET levels of UvrAB(K45A) with ATPγS (1.95) or ATP and CP/CK (1.73), however, are lower compared to those of the wild-type complex under the same conditions (2.29 and 1.95, respectively). This is most likely due to a reduced affinity of the UvrB(K45A) mutant for ATP, since this mutant lacks the amino acid responsible for interaction with the γ-phosphate of the ATP molecule. This again indicates that FRET is optimal when UvrB is in the ATP-bound form. With ATP in the absence of CP/CK, however, the opposite is observed where the level of FRET with UvrAB(K45A) is higher (1.62) than with the wild-type complex (1.44). This can be explained by the inability of UvrB(K45A) to hydrolyze ATP. With the wild-type complex, more ATP will be hydrolyzed and hence more ADP generated compared to UvrAB(K45A). As a consequence, more wild-type complexes will end up in the ADP-bound form which do not contribute to the FRET signal.

The Presence of Domain 4 Enhances the FRET Signal. To test whether the two UvrB molecules that bind to a UvrA dimer do interact via the domain 4 regions, we deleted this domain from the GFP2 and eYFP fusions (Figure 1). Deletion of domain 4 has been shown to result in a normal formation of the preincision complex but a defect in the UvrC interaction that is required for 3′ incision (*18*, *19*). As expected, the resulting UvrB635−GFP and −YFP fusion proteins are also no longer capable of supporting 3′ incision by UvrC (not shown), and 5′ incision on a prenicked substrate is comparable to that of a truncated UvrB without the GFP fusion (Figure 2). When the GFP2 and eYFP fusions of the UvrB635 truncation are combined with UvrA in the presence of ATPγS, a good FRET signal is again observed, but this signal is significantly lower compared to that of the full-length UvrB fusions (Figure 3C and Table 1). The spectra in the presence of ATP or ATP with CP/CK again show the effect of ATP hydrolysis on FRET, and also here, the magnitudes of the remaining signals with the UvrAB635 complex are reduced compared to those of the wtUvrAB complex. Apparently, in the wtUvrAB complex, GFP and YFP are closer to each other, most likely as a consequence of domain 4 dimerization.

Undamaged DNA Destabilizes the $UvrA_2B_2$ Complex. To test the effect of DNA on the observed FRET signal, we included the ATP-regenerating system in our incubation mixture. We have previously shown that at the relatively high protein and DNA concentrations used in spectroscopic measurements, the ATP hydrolysis is very high, and as a result, the available ATP becomes limiting (*21*). The addition of undamaged DNA to the UvrAB mixture resulted in a considerable decrease in the level of FRET in the case of both wtUvrB and UvrB635 (Figure 4A,B and Table 2). With the UvrB(K45A) mutant, however, an increase in the level of FRET is observed (Figure 4C and Table 2). The results shown are obtained using 1 μg of a mixture of linear DNA fragments (see Experimental Procedures), but identical results were found when an equal amount of nondamaged supercoiled pUC18 DNA was used (not shown). We interpret this result as follows. Within the $UvrA_2B_2$ complex, it is initially UvrA that detects potential damage in the DNA. When it hands the DNA over to UvrB, the ATPase site of UvrB is activated which is used to verify if damage is indeed present. When no damage is present, the ATP hydrolysis by UvrB leads to dissociation of the proteins from the DNA and to either complete or total dissociation of UvrB from the $UvrA_2B_2$ complex, and hence to disappearance of the FRET signal. This implies that the DNA-mediated dissociation of the $UvrA_2B_2$ complex is faster than the association of a new complex. In the UvrB(K45A) mutant, ATP hydrolysis is blocked, and therefore, the complex is trapped on the DNA, leading to a more stable $UvrA_2B_2$ complex compared to the complex in solution and, hence, an increase in the magnitude of the FRET signal.

We verified this model by determining the amount of protein−DNA complexes in a filter binding assay using exactly the same incubation mixture that was used for the FRET assay. Indeed, with wtUvrAB, only 6.5% of the undamaged DNA is retained on a filter, but in the presence of UvrA and UvrB(K45A), the extent of this binding is increased to 60% (Table 3).

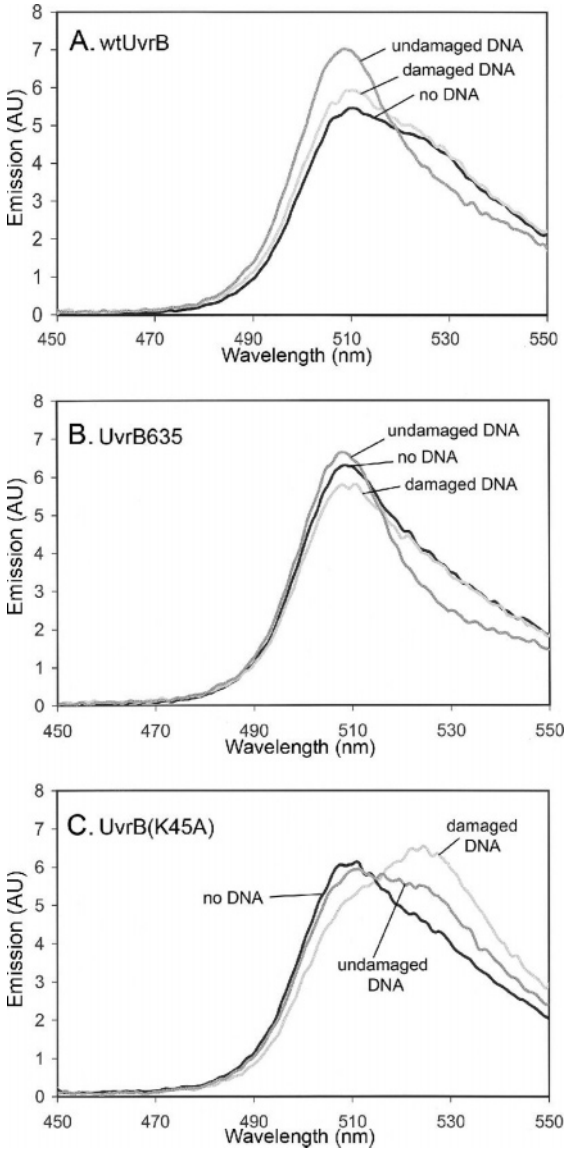

FIGURE 4: Emission spectra of the UvrB−GFP/UvrB−YFP pair in the presence of DNA. Incubation mixtures contained 2.5 pmol of UvrB−GFP, 22.5 pmol of UvrB−YFP, 25 pmol of UvrA, 1 mM ATP, and the ATP-regenerating system (CP/CPK): (A) UvrB−GFP and UvrB−YFP, (B) UvrB635−GFP and UvrB635−YFP, and (C) UvrB(K45A)−GFP and UvrB(K45A)−YFP. Spectra were recorded in the absence of DNA (black), with 1 μg of undamaged DNA (dark gray), or with 1 μg of UV-irradiated DNA. All spectra were corrected for direct YFP emission as described in the legend of Figure 3.

Table 2: Relative FRET Value of Proteins in the Presence of Undamaged or Damaged DNA[a]

	UvrAB	UvrAB(K45A)	UvrAB635
no DNA	1.95 ± 0.06	1.73 ± 0.04	1.52 ± 0.09
undamaged DNA	1.18 ± 0.02	2.20 ± 0.05	0.97 ± 0.03
UV-irradiated DNA	1.72 ± 0.03	3.01 ± 0.04	1.52 ± 0.05

[a] Measurements were taken in the presence of ATP and the CP/CK regenerating system.

Damage-Specific Binding of UvrB. Addition of UV-irradiated DNA to the incubation mixtures resulted in an increase in the magnitude of the FRET signal compared to those of the samples with nondamaged DNA for all UvrB variants that were tested (Figure 4 and Table 2). This must

Table 3: Filter Binding Assay

DNA	protein[a]	% binding
undamaged DNA	UvrA	2.2 ± 0.2
undamaged DNA	UvrAB	6.5 ± 0.3
undamaged DNA	UvrAB635	6.2 ± 0.2
undamaged DNA	UvrAB(K45A)	60.0 ± 1.7
UV-irradiated DNA	UvrA	2.6 ± 0.3
UV-irradiated DNA	UvrAB (5 pmol of UvrA)	58.9 ± 0.7
UV-irradiated DNA	UvrAB (12 pmol of UvrA)	57.8 ± 4.3
UV-irradiated DNA	UvrAB (25 pmol of UvrA)	58.3 ± 2.4
UV-irradiated DNA	UvrAB635 (25 pmol of UvrA)	69.2 ± 4.3
UV-irradiated DNA	UvrAB(K45A) (25 pmol of UvrA)	59.5 ± 3.4
UV-irradiated DNA	UvrABC(wt) (25 pmol of UvrA)	62.3 ± 3.3
UV-irradiated DNA	UvrABC(E81A) (25 pmol of UvrA)	63.1 ± 2.1
UV-irradiated DNA	UvrABC(D399A) (25 pmol of UvrA)	63.6 ± 2.5
UV-irradiated DNA	UvrABC(D399A) (12 pmol of UvrA)	63.7 ± 3.1

[a] The amount of each protein used is 25 pmol, unless stated otherwise.

Table 4: Effect of UvrA Concentration on FRET in the Presence of UV-Irradiated DNA

	wtUvrB	UvrB635
12 pmol of UvrA	1.55 ± 0.02	1.31 ± 0.02
25 pmol of UvrA	1.72 ± 0.03	1.52 ± 0.05
50 pmol of UvrA	1.98 ± 0.05	1.65 ± 0.04

reflect the damage-specific binding of a UvrB dimer on the DNA. Since in the assays mentioned above equimolar amounts of UvrA and UvrB (25 pmol) are used, it is possible that the damage-specific complexes that give rise to a FRET signal contain not only UvrB but also UvrA. To test this, we repeated the experiments with lower (12 pmol) or higher (50 pmol) UvrA concentrations. The results show that the strength of the FRET signal is proportional to the concentration of UvrA used, both for full-length UvrB and for the truncated form (Table 4). Twelve picomoles of UvrA should be enough to load UvrB on all the damaged sites (total of around 1 pmol). This was confirmed by a filter binding assay that shows that the amounts of damage-specific protein−DNA complexes using 25 pmol, 12 pmol, or even as little as 5 pmol of UvrA are the same (Table 3). Therefore, the decrease in the magnitude of the FRET signal with a lower UvrA concentration strongly suggests that the level of FRET is higher when UvrA is bound to the damage-specific UvrB−DNA complexes. There are two possible explanations for this UvrA-dependent FRET. First, it could mean that after dissociation of the UvrA protein one of the UvrB subunits also dissociates from the lesion. We regard this as being not very likely since AFM studies have shown that after dissociation of UvrA all of the damage-bound UvrB complexes contain two UvrB subunits (*14*). Alternatively, our data could indicate that after release of UvrA the GFP and YFP domains are separated by a longer distance, which would suggest that in the absence of UvrA the domain 4 regions do not stably interact. The relative amount of FRET for the B635 truncation is smaller compared to that of full-length UvrB (Table 2), although the level of damage-specific binding is even somewhat higher than with the wild-type proteins (Table 3). Again, the level of FRET with UvrB635 is dependent on the amount of UvrA used (Table 4). Apparently also in the absence of domain 4, the relative positions of the GFP and YFP proteins change (i.e., more close) when UvrA is associated with the damage-bound UvrB dimer. The reduced FRET value of the UvrB635 truncation compared to the full-length protein furthermore suggests that UvrA promotes domain 4 dimerization, not only in the UvrAB complex in solution but also on the DNA.

Table 5: Effect of UvrC on FRET in the Presence of UV-Irradiated DNA

UvrA	UvrB	UvrC	relative FRET
25 pmol of wt	25 pmol of wt	−	1.72 ± 0.03
25 pmol of wt	25 pmol of wt	25 pmol of E81A	1.71 ± 0.02
25 pmol of wt	25 pmol of wt	25 pmol of wt	1.93 ± 0.01
25 pmol of wt	25 pmol of wt	25 pmol of D399A	1.96 ± 0.05
25 pmol of wt	25 pmol of B635	−	1.52 ± 0.05
25 pmol of wt	25 pmol of B635	25 pmol of D399A	1.52 ± 0.03
12 pmol of wt	25 pmol of wt	−	1.55 ± 0.02
12 pmol of wt	25 pmol of wt	25 pmol of D399A	1.74 ± 0.03

We also assessed FRET with the UvrB(K45A) mutant in the presence of UV-damaged DNA (Figure 4C and Table 2). The relative FRET value is much higher than in the presence of undamaged DNA. This damage-related difference must mean that the mutant UvrAB complex is able to detect DNA damage. Filter binding assays, however, show that the amount of complexes formed by UvrAB(K45A) on DNA with or without UV damage are comparable (Table 3). Apparently, the damage-bound complexes are qualitatively different from the nondamaged ones, leading to a much higher level of FRET. This might again be related to the UvrA protein, which could remain more stably associated with UvrB on a damaged site than on nondamaged DNA.

UvrC Influences the FRET Signal. Next we looked at the FRET signal after addition of UvrA, UvrB, and UvrC (in equimolar amounts, i.e., 25 pmol). First, we used a UvrC mutant (E81A) which cannot incise the DNA due to a mutation in the 3′ catalytic site (ref *17* and unpublished observations from our lab). No significant difference in FRET is observed in presence or absence of this UvrC mutant (Table 5). However, when we used wtUvrC, or a UvrC deficient in 5′ incision only (D399A), FRET was significantly enhanced (Table 5). Apparently, the 3′ incision by UvrC is responsible for this increase. This is confirmed by the FRET assay with the UvrB635 truncation. In the absence of domain 4, UvrC is not capable of making the 3′ incision (*18*, *19*), and indeed, there is no difference in FRET signal after addition of UvrC to this truncated UvrB protein (Table 5). Furthermore, incubation of undamaged DNA with UvrA, UvrB, and UvrC(D399A) did not give rise to a significant FRET (1.09 ± 0.04), showing that the UvrC-mediated increase in the level of FRET is not due to stabilization of the $UvrA_2B_2$ complex on undamaged DNA or in solution.

When the assays with UvrC(D399A) were repeated using half the UvrA concentration (12 pmol), the amount of damage-specific complexes retained on a filter remained the same (Table 3) but the level of FRET is significantly reduced (Table 5). Apparently, also after incision, the FRET detected is largely due to the damage-bound UvrB dimers that are associated with UvrA, comparable to the FRET observed without UvrC. The fact that wtUvrC and UvrC(D399A) gave rise to a higher level of FRET and the 3′ catalytic mutant UvrC(E81A) did not indicates that UvrC does incise the DNA under the conditions used in our assays. It is, however, very unlikely that UvrC is capable of making the 3′ incision by binding to the $UvrA_2B_2$ complex. Incision by UvrC probably takes place when UvrA has dissociated from the

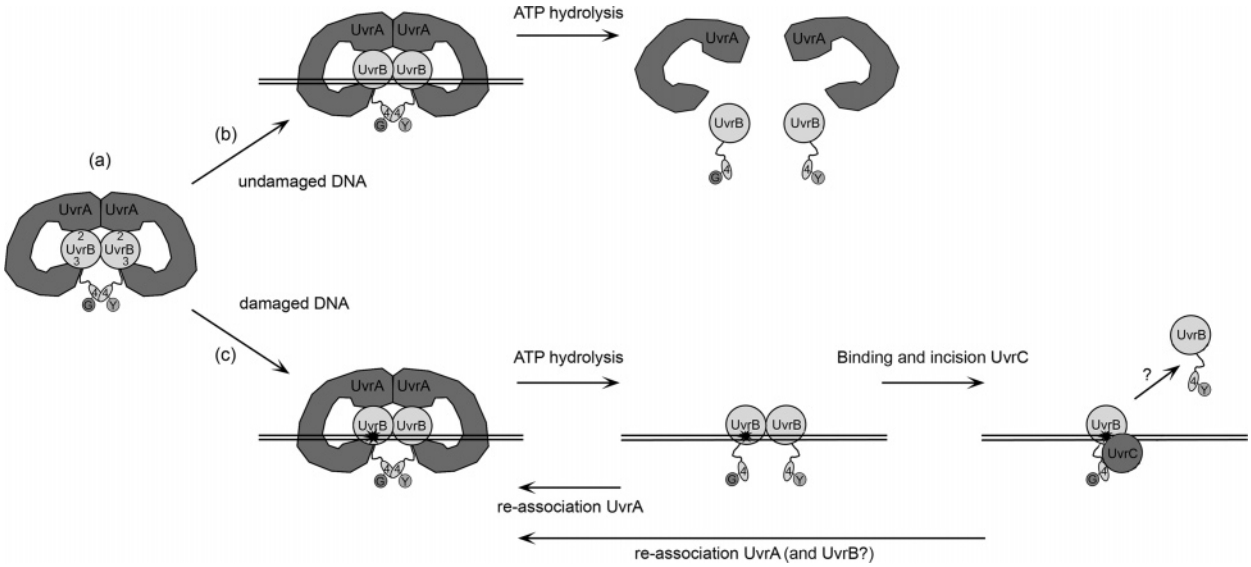

FIGURE 5: Model for the UvrA-dependent FRET of the UvrB dimer. (a) In the presence of ATP, a dimer of UvrA associates with two UvrB subunits. The binding of UvrA is mainly to domain 2 of the UvrB protein, but additional interaction with domain 3 and/or the linker region brings the two domain 4 regions closes together, allowing these regions to interact, thereby promoting FRET between the GFP (G) and YFP (Y) fusions. (b) Binding to undamaged DNA triggers the ATPase activity of UvrB, resulting in complete or partial dissociation of the complex and disappearance of FRET. (c) When the UvrB dimer binds to a site of DNA damage, ATP hydrolysis results in dissociation of the UvrA protein. As a result, the interaction between the two domain 4 regions is no longer stabilized, resulting in a reduction in the level of FRET. Only upon reassociation of UvrA is the contact between the domain 4 regions restored and can FRET again be detected. Binding of UvrC might cause dissociation of one of the UvrB subunits. After incision, UvrA (and UvrB) can reassociate to form the FRET-proficient complex again.

complex, and subsequently, UvrA reassociates after the incision to form the FRET-proficient $UvrA_2B_2$ complex again. The filter binding assay shows that formation of complexes on UV-damaged DNA in the presence of wtUvrC, UvrC(E81A), or UvrC(D399A) is comparable (Table 3), indicating that the enhanced FRET after incision is not due to a stabilizing effect of the incision on the overall interaction with the damaged site. The filter binding assay, however, does not discriminate between damage-bound UvrB monomers, UvrB dimers, and $UvrA_2B_2$ complexes. The enhanced FRET might therefore be the consequence of an enhanced reassociation of UvrA induced by a stabilizing effect of the nick in the DNA.

DISCUSSION

In this paper, we have analyzed the dimerization state of UvrB during the different steps of the repair reaction, by measuring the level of FRET between YFP and GFP fused to the C-terminal domain 4 region of the UvrB protein. In all the assays described in this study, a significant FRET can only be detected when UvrB is complexed with UvrA. This was apparent not only with the proteins in solution but also when they were bound to a DNA lesion and even after UvrC-mediated incision. From our results, we propose a model in which FRET is highly dependent on interaction between the domain 4 regions of two UvrB proteins and this interaction is promoted by the UvrA protein (Figure 5).

Gel filtration and cross-linking experiments have previously shown that UvrB in solution is a monomer at a concentration of 1 μM and a dimer at 5 μM (*13*). At the concentration of UvrB used in this study (0.4 μM), it is therefore very likely that in the absence of UvrA most of the UvrB is in the monomeric form. Addition of UvrA did result in significant FRET, showing, for the first time, that two UvrB molecules can bind to UvrA in solution most likely as part of a $UvrA_2B_2$ complex. The level of FRET in the $UvrA_2B_2$ complex is optimal when both UvrA and UvrB are in the ATP-bound form. It has been shown that dimerization of UvrA is stimulated by ATP (*12*). In the presence of ATPγS, the UvrA dimer was reported to be more stable than ATP, implying that ATP hydrolysis leads to monomerization of UvrA (*12*). In accordance, we find that the level of FRET of the $UvrA_2B_2$ complex is higher in the presence of ATPγS than ATP. It was also reported that UvrA forms stable dimers in the presence of ADP (*12*). In our study, however, we do not detect any FRET with ADP. Most likely, this is due to the inability of the UvrA dimer to interact with UvrB under these conditions because UvrA and/or UvrB is in the ADP-bound form. Indeed, Orren and Sancar (*11*) have shown that UvrA and UvrB cosediment in the presence of ATP but not in the presence of ADP. ATP hydrolysis by UvrB also leads to complete or partial dissociation of the $UvrA_2B_2$ complex which became clear from the enhanced FRET of the UvrAB-(K45A) complex compared to that of the wild-type complex. Most likely, the ATPase activities of UvrA and UvrB in solution reflect the ATP hydrolysis occurring on DNA when the complex is in search of damage.

When nondamaged DNA was added to wt $UvrA_2B_2$ complexes, FRET disappeared, whereas addition of DNA to a $UvrA_2B_2$ complex with a defective UvrB ATPase site (K45A) resulted in an increase in the level of FRET. Apparently, binding to nondamaged DNA triggers ATP hydrolysis in UvrB which in turn leads to dissociation of the $UvrA_2B_2$ complex, thereby disrupting FRET of the UvrB dimer (Figure 5). This dissociation is probably due to formation of an abortive complex where UvrA tries to hand over a putative damaged site to UvrB. The UvrB protein in

turn tries to bind the DNA, thereby hydrolyzing ATP, but fails to do so because of the lack of a DNA lesion. When ATP hydrolysis is not possible due to the K45A mutation, the complex is trapped on the DNA during this "hand-off" process. As a result, FRET in this trapped $UvrA_2B_2$ complex of the K45A mutant can still be observed. The DNA contacts in this complex apparently provide additional stabilization, causing a higher level of FRET of the mutant complex on the DNA compared to the proteins in solution.

UvrB bound to a lesion does give significant FRET, but again only when it is associated with UvrA. At lower UvrA concentrations, where the same amount of damage-specific protein−DNA complexes is formed, the level of FRET is decreased. It is not clear whether the residual FRET that is observed at lower UvrA concentrations is due to residual presence of UvrA in these complexes or to a remaining FRET in $UvrB_2$−DNA complexes that do not contain UvrA, but it is apparent that for optimal FRET UvrA binding is a prerequisite. As discussed above, handing over a damaged site to UvrB is accompanied by ATP hydrolysis in UvrB which triggers dissociation of UvrA, leaving UvrB bound to the damage. Since in this DNA-bound state UvrB has been shown to be able to bind ATP again (*31*), the UvrA protein can subsequently reassociate with the complex. This reassociation is highly dependent on the UvrA concentration, explaining the higher FRET levels with larger amounts of UvrA. AFM analysis of damage-bound UvrB complexes has shown that these complexes contain two UvrB molecules (*14*). Even after these complexes have been washed with buffer containing high salt to remove the UvrA protein, almost all complexes still have two UvrB molecules (*14*). This indicates that the reduced level of FRET after dissociation of UvrA is not due to monomerization of UvrB. We propose that in the absence of UvrA the two FRET partners are separated by too much to give efficient FRET (Figure 5). The Förster radius (distance at which FRET efficiency is 50%) of the GFP−YFP pair is 5.5 nm (*32*). The diameter of a UvrB monomer is between 5 and 9 nm. It is not known how the two monomers of UvrB are oriented in the dimer complex, but it is possible that they are oriented such that the GFP and YFP proteins are separated by ≥10 nm, which would be too far for detectable FRET.

One way by which UvrA could bring the FRET pair closer to each other is by promoting dimerization of the domain 4 regions of the two UvrB monomers. Indeed, in the absence of domain 4, the level of FRET of UvrAB complexes is reduced, both in solution and when bound to the DNA. The absence of domain 4 does not result in a reduction in the level of damage-specific binding of UvrB (refs *18* and *30* and this paper), showing that the overall affinity of UvrA for the truncated UvrB is not significantly reduced. Apparently, the higher level of FRET observed in the wild-type $UvrA_2B_2$ complex is caused because the domain 4 regions bring the GFP and YFP fusions closer together. It has been shown that interaction of UvrA with domain 2 of UvrB is critical for the formation of a productive UvrAB complex (*9*). A second UvrA binding domain in UvrB was identified with maltose-binding protein fusions which showed that UvrA interacts with the C-terminal region of UvrB from residue 547 to 673 (*10*). This includes domain 4 but also a part of domain 3 and the linker region between them. It is possible that the interaction with this C-terminal region brings the domain 4 regions of the UvrB monomers closer together, allowing them to interact (Figure 5). In the absence of domain 4, where GFP and YFP are directly fused to the linker region, the same contact of UvrA with domain 3 and/or the linker region will also bring the GFP and YFP physically closer, explaining why for the truncated protein FRET is still observed in the presence of UvrA.

It has been proposed, on the basis of experiments with *Bacillus caldotenax* UvrB, that interaction of UvrA with the C-terminal part of UvrB regulates the ATPase activity of UvrB by repositioning domain 4 relative to the other domains of the UvrB protein, thereby altering the ATP binding pocket (*30*). We propose that this repositioning at the same time promotes dimerization of the domain 4 regions which might serve another function, shielding of this domain for UvrC binding. For 3′ incision to occur, domain 4 needs to interact with a homologous internal domain of UvrC (*18*, *19*). As long as UvrA is bound to UvrB, e.g., during the search for and verification of a damaged site, the domain 4 regions dimerize, preventing premature binding and incision by UvrC. Only after binding of UvrB to a damaged site and subsequent dissociation of UvrA is this dimerization destabilized, allowing recruitment of UvrC.

After addition of UvrC to the damage-bound complexes, FRET could still be observed, but again in a UvrA-dependent way. A UvrC that is proficient in 3′ incision gave rise to an even higher level of FRET. It is generally believed that prior to UvrC incision UvrA dissociates from the UvrB−DNA complex, which is mainly based on the observation that catalytic amounts of UvrA can load UvrB on all damaged sites (*11*) and that purified UvrB−DNA complexes that no longer contain UvrA can be incised by UvrC (*11*, *31*). It was also proposed on the basis of footprint data and AFM analysis that upon binding of UvrC one of the UvrB subunits dissociates from the damage-bound dimer (*14*, *15*). From the results presented in this paper, we cannot determine whether the second UvrB subunit is displaced by UvrC since apparently after incision the $UvrA_2B_2$−DNA complex is reconstituted in such an efficient way that a UvrC-mediated dissociation of UvrB which would lead to reduction of FRET cannot be detected. Since the level of FRET is increased with UvrC proteins that results in 3′ (D399A) or 3′ and 5′ (wt) incisions, the reassociation of UvrA and/or the second UvrB subunit even seem to be enhanced by the presence of a nick in the DNA. It is possible that the nick in the DNA provides an additional contact for the UvrA protein, thereby stabilizing the $UvrA_2B_2$ complex.

Reassociation of UvrA with damage-specific UvrB−DNA complexes after incision has been shown before by Visse et al. (*33*). In these experiments, damaged DNA was incubated with UvrA, UvrB, and UvrC, after which the UvrAB−DNA and UvrB−DNA complexes were separated and purified from a gel. Analysis of the DNA in these complexes subsequently indicated that the DNA not only in the UvrB−DNA complex but also in the UvrAB−DNA complex had been incised, showing that UvrA can reassociate with the UvrB−DNA complex after incision. Whether this reassociation of UvrA also occurs in vivo remains to be determined. Possibly UvrD and/or PolI will prevent binding of UvrA after incision. On the other hand, the UvrA reassociation might serve a good purpose if in this way UvrA again shields the

domain 4 regions, thereby preventing rebinding of UvrC to complexes that have already been incised.

ACKNOWLEDGMENT

We thank John van Dam and Erik van Driel for technical assistance in constructing and purifying the GFP and YFP fusion proteins.

REFERENCES

1. Goosen, N., and Moolenaar, G. F. (2001) Role of ATP hydrolysis by UvrA and UvrB during nucleotide excision repair, *Res. Microbiol. 152*, 401−409.
2. Van Houten, B., Croteau, D. L., DellaVecchia, M. J., Wang, H., and Kisker, C. (2005) 'Close-fitting sleeves': DNA damage recognition by the UvrABC nuclease system, *Mutat. Res. 577*, 92−117.
3. Truglio, J. J., Croteau, D. L., Van Houten, B., and Kisker, C. (2006) Prokaryotic nucleotide excision repair: The UvrABC system, *Chem. Rev. 106*, 233−252.
4. Theis, K., Chen, P. J., Skorvaga, M., Van Houten, B., and Kisker, C. Crystal structure of UvrB, a DNA helicase adapted for nucleotide excision repair, *EMBO J. 18*, 6899−6907.
5. Machius, M., Henry, L., Palnitkar, M., and Deisenhofer, J. (1999) Crystal structure of the DNA nucleotide excision repair protein UvrB from *Thermus thermophilus*, *Proc. Natl. Acad. Sci. U.S.A. 96*, 11717−11722.
6. Nakagawa, N., Sugahara, M., Masui, R., Kato, F., Fukuyama, K., and Kuramitsu, S. (1999) Crystal structure of *Thermus thermophilus* HB8 UvrB protein, a key enzyme of nucleotide excision repair, *J. Biochem. 126*, 986−990.
7. Sohi, M., Alexandrovich, A., Moolenaar, G. F., Visse, R., Goosen, N., Vernede, X., Fontecilla-Camps, J. C., Champness, J., and Sanderson, M. R. (2000) Crystal structure of *Escherichia coli* UvrB C-terminal domain and a model for UvrB-UvrC interaction, *FEBS Lett. 465*, 161−164.
8. Alexandrovich, A., Sanderson, M. R., Moolenaar, G. F., Goosen, N., and Lane, A. N. (1999) NMR assignments and secondary structure of the UvrC binding domain of UvrB, *FEBS Lett. 451*, 181−185.
9. Truglio, J. J., Croteau, D. L., Skorvaga, M., DellaVecchia, M. J., Theis, K., Mandavilli, B. S., Van Houten, B., and Kisker, C. (2004) Interactions between UvrA and UvrB: The role of UvrB's domain 2 in nucleotide excision repair, *EMBO J. 23*, 2498−2509.
10. Hsu, D. S., Kim, S. T., Sun, Q., and Sancar, A. (1995) Structure and function of the UvrB protein, *J. Biol. Chem. 270*, 8319−8327.
11. Orren, D. K., and Sancar, A. (1989) The (A)BC excinuclease of *Escherichia coli* has only the UvrB and UvrC subunits in the incision complex, *Proc. Natl. Acad. Sci. U.S.A. 86*, 5237−5241.
12. Oh, E. Y., Claassen, L., Thiagalingam, S., Mazur, S., and Grossman, L. (1989) ATPase activity of the UvrA and UvrAB protein complexes of the *Escherichia coli* UvrABC endonuclease, *Nucleic Acids Res. 17*, 4145−4159.
13. Hildebrand, E. L., and Grossman, L. (1999) Oligomerization of the UvrB nucleotide excision repair protein of *Escherichia coli*, *J. Biol. Chem. 274*, 27885−27890.
14. Verhoeven, E. E. A., Wyman, C., Moolenaar, G. F., and Goosen, N. (2002) The presence of two UvrB subunits in the UvrAB complex ensures damage detection in both DNA strands, *EMBO J. 21*, 4196−4205.
15. Moolenaar, G. F., Schut, M., and Goosen, N. (2005) Binding of the UvrB dimer to non-damaged and damaged DNA: Residues Y92 and Y93 influence the stability of both subunits, *DNA Repair 4*, 699−713.
16. Verhoeven, E. E. A., van Kesteren, M., Moolenaar, G. F., Visse, R., and Goosen, N. (2000) Catalytic sites for 3′- and 5′-incision of *E. coli* nucleotide excision repair are both located in UvrC, *J. Biol. Chem. 275*, 5120−5123.
17. Truglio, J. J., Rhau, B., Croteau, D. L., Wang, L., Skorvaga, M., Karakas, E., DellaVecchia, M. J., Wang, H., Van Houten, B., and Kisker, C. (2005) Structural insights into the first incision reaction during nucleotide excision repair, *EMBO J. 24*, 885−894.
18. Moolenaar, G. F., Franken, K. L., Dijkstra, D. M., Thomas-Oates, J. E., Visse, R., van de Putte, P., and Goosen, N. (1995) The C-terminal region of the UvrB protein of *Escherichia coli* contains an important determinant for UvrC binding to the preincision complex but not the catalytic site for 3′-incision, *J. Biol. Chem. 270*, 30508−30515.
19. Moolenaar, G. F., Franken, K. L., van de Putte, P., and Goosen, N. (1997) Function of the homologous regions of the *Escherichia coli* DNA excision repair proteins UvrB and UvrC in stabilization of the UvrBC-DNA complex and in 3′-incision, *Mutat. Res. 385*, 195−203.
20. Zimmermann, T., Rietdorf, J., Girod, A., Georget, V., and Pepperkok, R. (2002) Spectral imaging and linear un-mixing enables improved FRET efficiency with a novel GFP2-YFP FRET pair, *FEBS Lett. 531*, 245−249.
21. Malta, E., Moolenaar, G. F., and Goosen, N. (2006) Base flipping in nucleotide excision repair, *J. Biol. Chem. 281*, 2184−2194.
22. Moolenaar, G. F., Visse, R., Ortiz-Buysse, M., Goosen, N., and van de Putte, P. (1994) Helicase motifs V and VI of the *Escherichia coli* UvrB protein of the UvrABC endonuclease are essential for the formation of the preincision complex, *J. Mol. Biol. 240*, 294−307.
23. Moolenaar, G. F., Höglund, L., and Goosen, N. (2001) Clue to damage recognition by UvrB: Residues in the β-hairpin structure prevent binding to non-damaged DNA, *EMBO J. 20*, 6140−6149.
24. Visse, R., de Ruijter, M., Moolenaar, G. F., and van de Putte, P. (1992) Analysis of UvrABC endonuclease reaction intermediates on cisplatin-damaged DNA using mobility shift gel electrophoresis, *J. Biol. Chem. 267*, 6736−6742.
25. Verhoeven, E. E. A., van Kesteren, M., Turner, J. J., van der Marel, G. A., van Boom, J. H., Moolenaar, G. F., and Goosen, N. (2002) The C-terminal region of *E. coli* UvrC contributes to the flexibility of the UvrABC nucleotide excision repair system, *Nucleic Acids Res. 30*, 2492−2500.
26. Douki, T., Court, M., Sauvaigo, S., Odin, F., and Cadet, J. (2000) Formation of the main UV-induced thymine dimeric lesions within isolated and cellular DNA as measured by high performance liquid chromatography-tandem mass spectrometry, *J. Biol. Chem. 275*, 11678−11685.
27. Sambrook, J., Fritsch, E. F., and Maniatis, T. (1989) in *Molecular Cloning: A Laboratory Manual*, Cold Spring Harbor Laboratory Press, Plainview, NY.
28. Verhoeven, E. E. A., van Kesteren, M., Turner, J. J., van der Marel, G. A., van Boom, J. H., Moolenaar, G. F., and Goosen, N. (2002) The C-terminal region of *Escherichia coli* UvrC contributes to the flexibility of the UvrABC nucleotide excision repair system, *Nucleic Acids Res. 30*, 2492−2500.
29. Seeley, T. W., and Grossman, L. (1989) Mutations in the *Escherichia coli* UvrB ATPase motif compromise excision repair capacity, *Proc. Natl. Acad. Sci. U.S.A. 86*, 6577−6581.
30. Wang, H., DellaVecchia, M. J., Skorvaga, M., Croteau, D. L., Erie, D. A., and Van Houten, B. (2006) UvrB domain 4, an autoinhibitory gate for regulation of DNA binding and ATPase activity, *J. Biol. Chem. 281*, 15227−15237.
31. Moolenaar, G. F., Herron, M. F., Monaco, V., van der Marel, G. A., van Boom, J. H., Visse, R., and Goosen, N. (2000) The role of ATP binding and hydrolysis by UvrB during nucleotide excision repair, *J. Biol. Chem. 265*, 8044−8050.
32. Ameer-Beg, S. M., Edme, N., Peter, M., Barber, P. R., Ng, T., and Vojnovic, B. (2003) Imaging protein-protein interactions by multiphoton FLIM, *Proc. SPIE 5139*, 180−189.
33. Visse, R., de Ruijter, M., Moolenaar, G. F., and van de Putte, P. (1991) Analysis of UvrABC endonuclease intermediates on cisplatin-damaged DNA using mobility shift gtel electrophoresis. *J. Biol. Chem. 267*, 6736−6742.

BI7002235